



iJRASET

International Journal For Research in
Applied Science and Engineering Technology



INTERNATIONAL JOURNAL FOR RESEARCH

IN APPLIED SCIENCE & ENGINEERING TECHNOLOGY

Volume: 5 Issue: VIII Month of publication: August 2017

DOI: <http://doi.org/10.22214/ijraset.2017.8267>

www.ijraset.com

Call:  08813907089

E-mail ID: ijraset@gmail.com

Solid State Transformer in Wind Energy Conversion System with Hybrid Renewable Energy System

I. Prabhu Kiran Immanuel¹, B. Mohan²

¹M.Tech Student Scholar, ²M.Tech, Assistant Professor

Department of Electrical & Electronics Engineering,

PVP Siddhartha Engineering College, Kanuru, Vijayawada, Krishna (Dt), AP, India.

Abstract: Wind power is presently one of the most rapidly increasing renewable energy sources. As a result of the wind power being an uncontrollable resource, various problems regarding power quality and protection issues generate. The solid-state transformer (SST) has been found to be useful in integration of different distributed energy sources as well as wind power in the distribution grid with multiple functionalities. A wind-solar hybrid system using solid state transformer (SST) for reactive power compensation to achieve power quality as per IEC standards. The proposed hybrid system using SST can effectively suppress the voltage fluctuation. This work proposes a new modelling approach of a combined Photovoltaic and Wind power system. This paper proposes a configuration that combines the doubly fed induction generator (DFIG) based wind turbine and SST operation in the presence of MATLAB/SIMULINK Software.

KeyWords: Doubly Fed Induction Generator, Fault Ride Through, Hybrid Renewable Energy System, PV System, Solid State Transformer, Wind Energy.

I. INTRODUCTION

With the random increment of power demand, the amount of renewable energy integration into the conventional grid is increasing day by day. The interest in renewable sources of energy has increase, considerably. They represent a potential solution to mitigate environmental issues and reduce the dependence on traditional sources of energy for electrical generation [1-4]. The need of technology for adapting these non-traditional types of energy into the system has motivated the development of new generation power electronics converters. The future homes will make use of power converters to integrate all the available sources of electrical energy, including renewables as wind turbine (WT) and PV. Photovoltaic's (PV) is a method of generating electrical power by converting solar radiation into direct current electricity using semiconductors that exhibit the photovoltaic effect. Photovoltaic power generation employs solar panels composed of a number of solar cells containing a photovoltaic material. Photovoltaic are best known as a method for generating electric power by using solar cells to convert energy from the sun into a flow of electrons [5]. Wind Energy Conversion Systems (WECS) constitute a mainstream power technology that is largely under exploited. The main differences in WECS technology are in electrical design and control [6]. At present, typically two types of WECS for large wind turbines exists. The first one is a variable speed WECS that allows variable speed operation over a large, but still restricted, range. This type of WECS mainly uses a Doubly Fed Induction Generator (DFIG) with the stator windings connected directly to the three phase constant – frequency grid and the rotor windings connected to a partial scale back to back converter. A multi stage gear box is necessary in this drive [7-9]. This type of WECS offer high controllability, smoother grid connection, maximum power extraction and reactive power compensation using back to back power converters of rating near to 25-30% of the generator capacity.

SST are composed of mainly power electronics based components can also be referred to as a type of power device. These devices are extremely effective in regulating the magnitude of voltage, current or frequency according to the application wise requirements [10]. Solid State Transformer functionalities protects the load from power supply disturbances, Voltage Harmonics and sag compensations Outage compensation, Protects power systems from the load disturbances, Load transients and harmonic regulations, Unity input power factor under reactive load, Sinusoidal input current for nonlinear loads, Protection against output short circuit, Operates on distributed voltage level, Integrates energy storage, Medium frequency isolation [11]. As seen in Fig. 1, SST can act as an interface between the grid and generation sources. In this paper, a new configuration is proposed that combines the operation of Photovoltaic and DFIG based WECS and SST [12][13]. This configuration acts as an interface between the wind turbine and grid while eliminating the GSC of DFIG. Moreover, it is essential to have fault ride through (FRT) incorporated in DFIG system to meet

the grid code requirements. In the proposed work, the developed configuration allows DFIG to ride through faults seamlessly. The total system operation is implemented on MATLAB/SIMULINK platform.

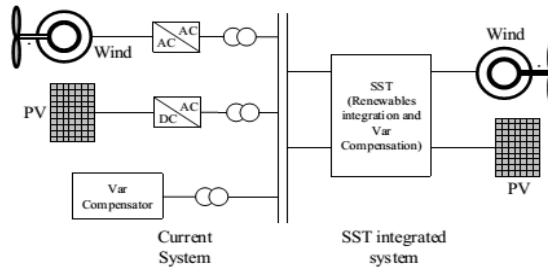


Fig.1 Expected SST integrated grid

II. PROPOSED SYSTEM CONFIGURATION AND MODELING

A. Motivation for DFIG

It has been reported that a DFIG based wind turbine is the lightest amongst the current wind systems which also explains its wide commercial use. Moreover, in the proposed configuration, the GSC present in traditional DFIG systems is removed making the machine setup further lighter. On the other hand, SST being used in an AC/AC system is expected to be 25% smaller in volume than traditional low frequency transformer. Thus, the use of SST to interface a DFIG based wind system can be expected to provide further reduction in weight and volume when compared to other wind systems with the fundamental frequency transformer.

B. DFIG Configuration

The widely used DFIG based WECS configuration is shown in Fig.2(a). The stator terminals of the machine are connected directly to the grid while the rotor terminals are connected via back to back converters. The RSC allows for variable speed operation of the machine by injecting or drawing active power from the rotor. The GSC maintains the DC link by transferring the active power from the rotor to the grid or vice versa. The step up transformer T1, is the interface between the DFIG system and grid.

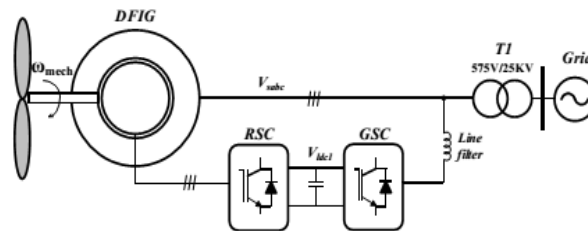


Fig.2 (a) Regular DFIG configuration

Three stage SST configuration is shown in Fig.2 (b), where it connects the grid to a distribution load. Conv-1 is a fully controlled three-phase converter connected to the high voltage grid (11-33 kV). It draws real power from the grid and maintains the high voltage DC bus (v_{dc}). This high voltage DC is converted to high frequency AC voltage by a half bridge converter (HB-1) which is then stepped down using a smaller sized high frequency transformer. This transformer provides the galvanic isolation between the grid and load. A second half bridge converter (HB-2) converts the low voltage AC to low voltage DC voltage (v_{dc}). This DC bus supports conv-2 which maintains the three-phase/single phase supply voltage to the load by producing a controlled three phase voltage. The configuration thus performs the function of a regular transformer allowing for bi-directional power flow using a series of power electronics devices.

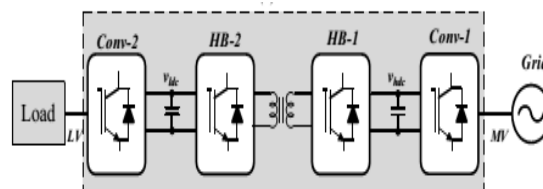


Fig.2 (b) SST structure

without requiring any additional control or device. Furthermore, the GIC can provide reactive power support to the grid during low wind generation periods.

D. DFIG Modeling

The DFIG is modeled using the *d-q* synchronous reference frame rotating at synchronous speed. The machine flux equations can be written in the *d-q* reference frame as,

$$\left. \begin{aligned} \lambda_{sd} &= L_{ls}i_{sd} + L_m(i_{sd} + i_{rd}) \\ \lambda_{sq} &= L_{ls}i_{sq} + L_m(i_{sq} + i_{rq}) \\ \lambda_{rd} &= L_{lr}i_{rd} + L_m(i_{sd} + i_{rd}) \\ \lambda_{rq} &= L_{lr}i_{rq} + L_m(i_{sq} + i_{rq}) \end{aligned} \right\} \quad (1)$$

The voltage equations for the stator and rotor are given as,

$$\left. \begin{aligned} v_{sd} &= r_s i_{sd} - \omega \lambda_{sq} + \frac{d\lambda_{sd}}{dt} \\ v_{sq} &= r_s i_{sq} - \omega \lambda_{sd} + \frac{d\lambda_{sq}}{dt} \\ v_{rd} &= r_r i_{rd} - (\omega - \omega_r) \lambda_{rq} + \frac{d\lambda_{rd}}{dt} \\ v_{rq} &= r_r i_{rd} (\omega - \omega_r) \lambda_{rd} + \frac{d\lambda_{rq}}{dt} \end{aligned} \right\} \quad (2)$$

The *d* and *q* axes quantities are represented by the respective subscripts *d* and *q*. *r_s* and *r_r* represent the stator and rotor resistances. *L_{ls}*, *L_{lr}* and *L_{lm}* represent the stator, rotor and mutual inductances referred to stator. ω represents the electrical supply frequency and ω_r represents the rotor frequency. Using (1)-(2), the torque equation for the machine can be obtained as,

$$T = -\frac{\lambda_{sd} L_m}{L_s} i_{qr} \quad (3)$$

It can be understood from the above equation that on aligning the stator flux with the *d*-axis, the torque in the machine can be controlled by varying *i_{qr}*. This is the basis on which the rotor side converter is controlled. It can also be shown that by varying *i_{dr}*, reactive power output from the stator can be controlled. Further details on the DFIG modeling can be obtained from.

III. CONTROL OF THE PROPOSED SYSTEM

To ensure smooth operation of the proposed configuration, the control objectives and algorithms for the RSC, MIC and the GIC are discussed below and shown in Fig.4.

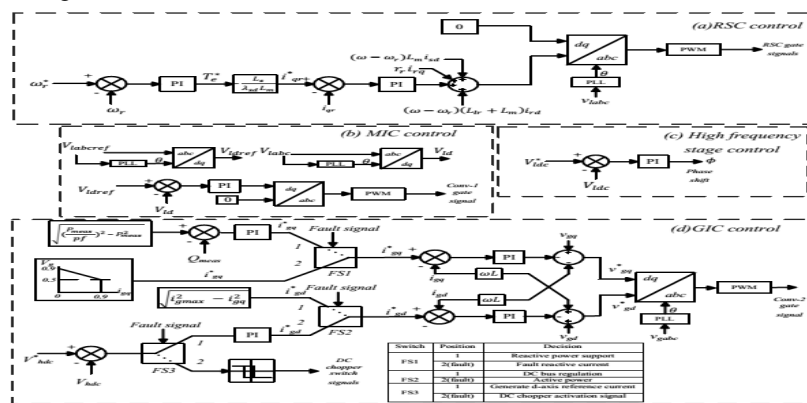


Fig.4. Control diagram of proposed configuration.

A. RSC Control

The rotor side control ensures the variable speed operation of DFIG by enabling the generator to work in super synchronous or sub synchronous modes. In super synchronous mode, the total power generated is partially evacuated through the RSC. Under sub synchronous modes, the RSC injects active power into the rotor. The RSC in the proposed converter is controlled using a decoupled synchronous frame reference. The *d*-axis of the reference frame is aligned with the machine stator voltage. On doing this, as per (3), the torque produced by the machine can be directly controlled by controlling the *d*-axis rotor current *i_{qr}*. Moreover, the reactive power produced at the stator terminal can also be controlled by controlling the *d*-axis rotor current *i_{dr}*. The control schematic for the same is shown in Fig.4. A suitable MPPT curve is used to track the optimal rotor speed and is compared with the

measured rotor speed. The error is processed by a PI controller to produce the reference torque (T_e^*) for the machine. Using (3.3), the rotor d-axis reference current (i_{qr}^*) is calculated. This current is compared with the actual rotor q-axis current (i_{qr}) and the error is processed by a PI controller to generate the q-axis reference voltage (v_{qr}^*). In the proposed configuration, the stator terminals are completely decoupled from the grid through the SST. The GIC supplies any reactive power requirement from the grid and the machine only generates active power. This eliminates the need for control over d-axis the rotor current and voltage. Thus, the d-axis rotor voltage reference for RSC (v_{dr}^*) is maintained as zero. The d-q axis reference voltages are then converted to three phase and used to generate the gate pulses for the RSC. Further details regarding the control system can be obtained.

B. MIC Control

The MIC is the first stage of the SST connecting the low voltage machine output to the high frequency stage. This converter is controlled to maintain 1 p.u. voltage (0.575 kV) at 50 Hz at the stator terminals of the machine.

The control is achieved by generating a reference voltage and comparing the d-axis component of the reference (v_{sd}^*) with the voltage at the output of the converter (v_{sd}). The power generated at the stator terminals of the machine is thus absorbed by the low voltage DC bus connected to MIC operating at 1.15 kV.

C. High Frequency Stage Control

The high frequency stage transforms the low voltage DC bus voltage (1.15 kV) into high voltage DC (50 kV). The DC voltages are converted into high frequency AC voltages by the two half bridge converters. Power is transferred by introducing a phase shift between the AC voltages of the two converters linked together by a high frequency transformer. The equation that governs the transfer of power is given as,

$$P = \frac{v_{hdc} v_{ldc} \phi (\pi - \phi)}{2\pi \omega L_k \pi} \quad (4)$$

Where ϕ is the phase shift between the AC voltages and L_k is the leakage inductance of the high frequency transformer. The complete derivation of the power transfer equation and further details can be obtained. The control objective of high frequency stage, in the proposed configuration, is to maintain the low voltage DC bus voltage (v_{ldc}) at a constant level. In order to achieve this, the reference voltage is v_{ldc}^* compared with the measured value and the resulting error is processed by a PI controller which produces the required phase shift ϕ that transfers the active power from the low voltage DC bus to the high voltage DC bus. The schematic for control is shown in Fig.4 (c).

D. GIC control

While the control of other converters remains the same in fault and normal conditions, GIC is controlled differently during fault conditions. The control and operation of GIC is discussed in two modes. Fault detection switches are used that are triggered when a fault is detected. The positions of the switches and their operation are summarized in a table in Fig.4 (d).

- 1) *Normal Mode* : Under normal mode of operation, the objective of the GIC is to ensure that the active power produced by the wind system is delivered to the grid. Additionally, it is suggested in this paper that the GIC provide reactive support as per user defined power factor to the grid when the wind generation is lower than rated value. Fig.4 (d) shows the overall control of GIC. The control of the converter is designed based on the d-q reference frame. The d-axis current (i_{gd}) controls the flow of active power and the DC bus voltage while the q-axis current (i_{gq}) controls the reactive power flow. The q-axis reference grid current (i_{gq}^*) is generated based on the user defined power factor requirement which is used to calculate the reference reactive power (Q^*) which is compared with the measured reactive power (Q_{meas}) and passed through a PI controller. Reference reactive power Q^* can be calculated from the power factor as

$$Q^* = \sqrt{\left(\frac{P_{meas}}{pf}\right)^2 - P_{meas}^2} \quad (5)$$

The d-axis reference current is generated by passing the error between the measured DC bus voltage and its reference through a PI controller. An outer loop voltage controller then generates the d-axis reference voltage v_{gd}^* . Similarly, the q-axis reference voltage v_{gq}^* is obtained from a PI controller on the q-axis current.

- 2) *Fault Mode* : The objective of the GIC under fault conditions is to supply the reactive currents as per the grid codes. The fault in the system is identified by monitoring the positive sequence grid voltage which is effective in both symmetrical and unsymmetrical fault conditions.

Upon identifying the fault, the fault switches (FS1 to FS3) shown in Fig.4 (d) are activated. Under fault conditions, preference is given to reactive current injection and the control of DC bus by the GIC is deactivated by FS3. The reactive current reference enabled by FS2 for the GIC is generated as per the grid codes shown in Fig.3.5 and is calculated as,

$$\frac{\Delta i}{i_n} = i_{gp}^* = \begin{cases} \left(\frac{\Delta v}{v_n}\right) * \frac{1}{0.5} & \text{if } 1 > \frac{\Delta v}{v_n} > 0.5 \\ 1 \text{ p.u.} & \text{if } 0.5 > \frac{\Delta v}{v_n} > 0 \end{cases} \quad (6)$$

Where Δv , is the difference between the pre-fault voltage and the current grid voltage and v_n is the rated nominal voltage. Δi Is the difference between the pre-fault reactive current and the reactive current during fault and i_n is the rated current value. In the case considered in this paper i_n is 1 p.u. And there is no pre-fault reactive current, thus, $\frac{\Delta i}{i_n}$ is equal to the reactive current to be injected i.e. i_{gp}^* . Recent grid codes in some countries have even more aggressive reactive current requirements sometimes requiring the wind farm to supply up to 1.2 p.u. reactive currents. The q-axis reference current is then compared with the measured one. The error is processed by a PI controller to generate the q-axis reference voltage (v_{qr}^*). When the fault is less severe and the voltage dip is less than 1 p.u. the grid codes do not impose any restriction on injecting active power into the grid. Hence, after prioritizing reactive current injection, the remaining capacity of the GIC is used to continue to inject any active power possible by switching FS1. The reference for the d-axis current is generated as follows based on the maximum allowable rating of the GIC, i_{gmax} and is expressed as

$$i_{gd}^* = \sqrt{i_{gmax}^2 - i_{gp}^2} \quad (7)$$

Upon identification of fault, in order to prevent the DC bus voltage from rising, a DC chopper is employed (FS3 at position 2). The measured error between the high voltage DC bus reference (v_{hdc}^*) and the measured value (v_{hdc}) is passed through a hysteresis relay that produces the switching signal for DC chopper circuit. Which is designed to allow for a two percent variation in bus voltage.

$$S1 = \begin{cases} ON & \text{if } v_{hdc}^* - v_{hdc} > 1 \text{ KV} \\ OFF & \text{if } v_{hdc}^* - v_{hdc} < 1 \text{ KV} \end{cases} \quad (8)$$

IV. HYBRID RENEWABLE ENERGY SYSTEMS

Hybrid energy system is including several (two or more) energy sources with appropriate energy conversion technology connected together to feed power to local load/grid. Figure 4.1 gives the general pictorial representation of Hybrid energy system. Since, it is coming under distributed generation system; there is no unified standard or structure. It receives benefits in terms of reduced line and transformer losses, reduced environmental impacts, relived transmission and distribution congestion, increased system reliability, improved power quality, peak shaving, and increased overall efficiency.

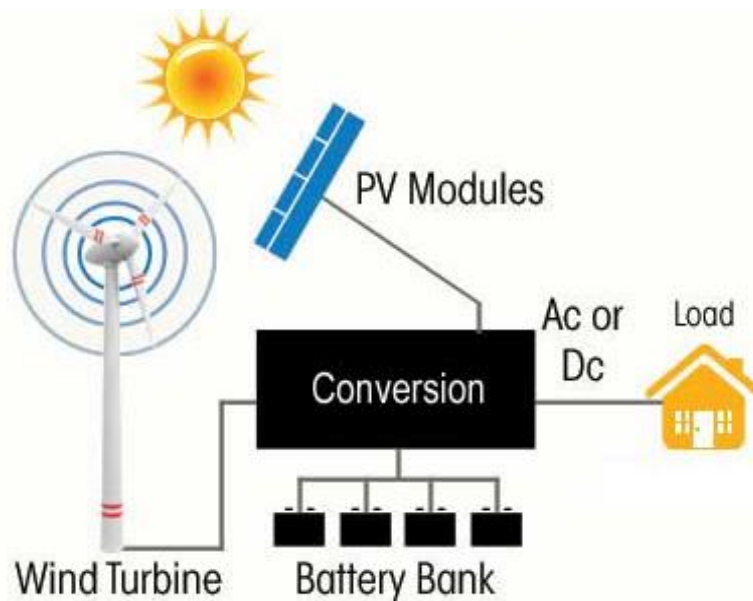


Fig.5 Hybrid Renewable Energy System

V. MATLAB/SIMULINK RESULTS

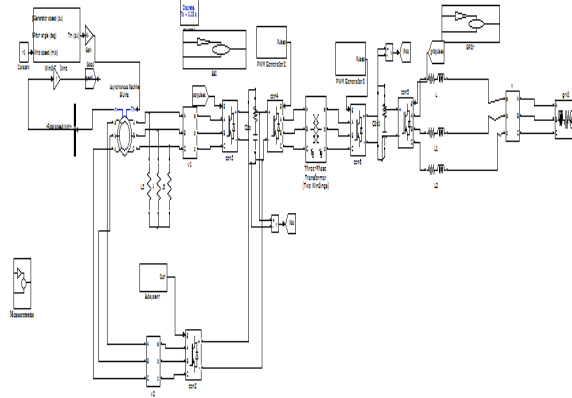
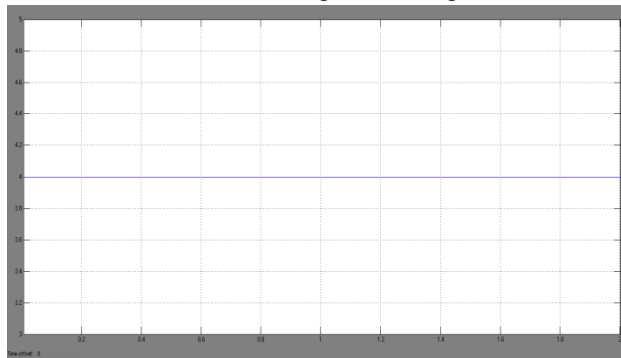
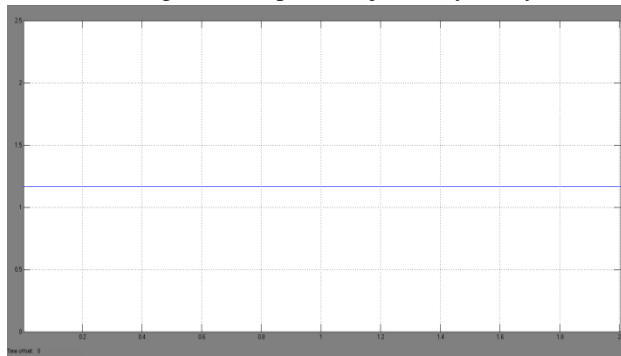


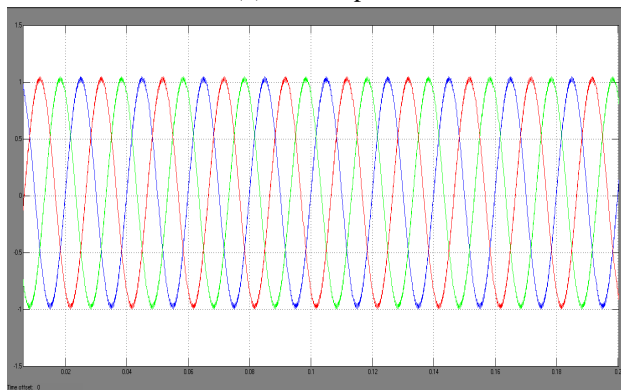
Fig 6 MATLAB/Simulink circuit diagram for Regular DFIG configuration



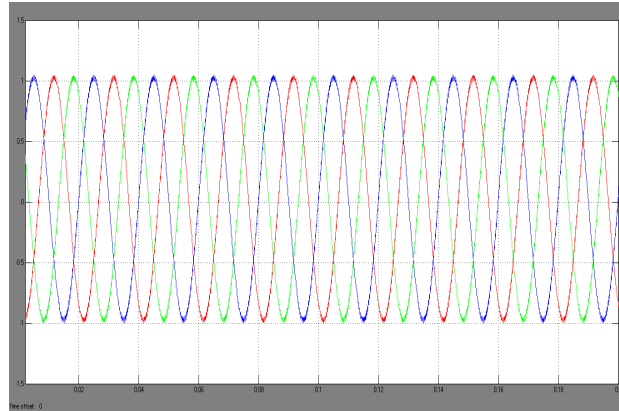
(a) Pgen active power injected by the system



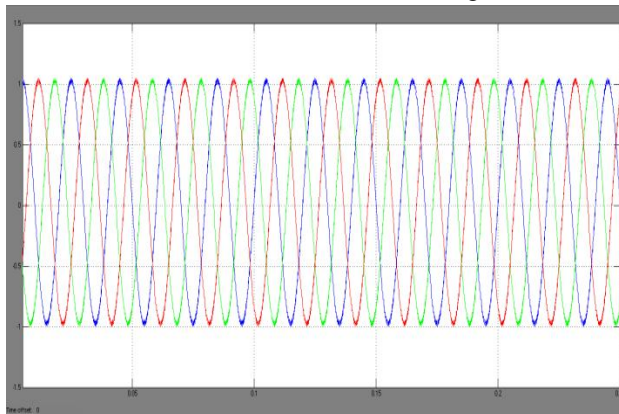
(b) Rotor Speed



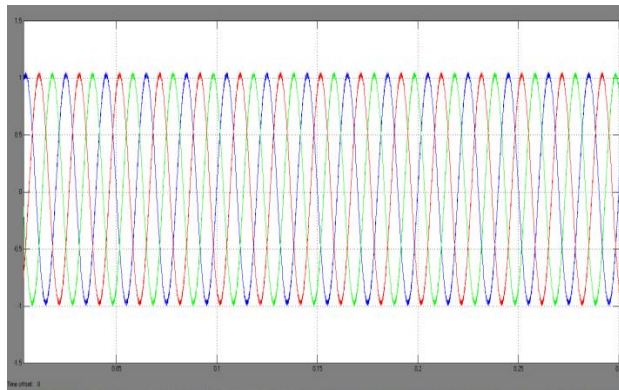
(c) Vgabc Grid voltages



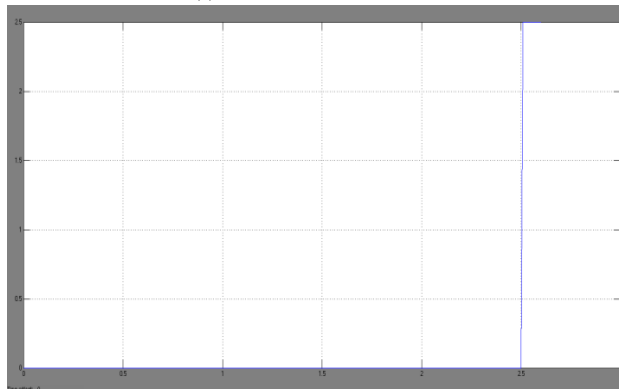
(d) Vsabc stator terminal voltages



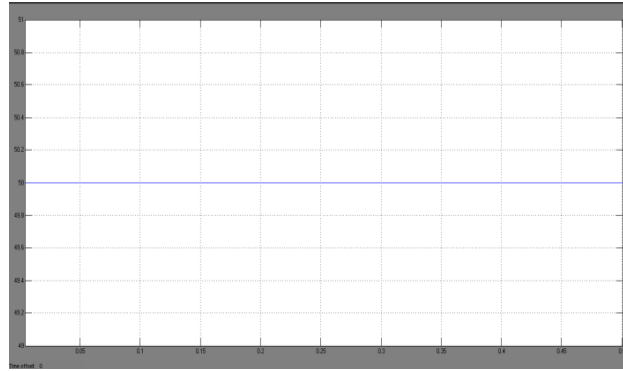
(e) Igabc grid currents



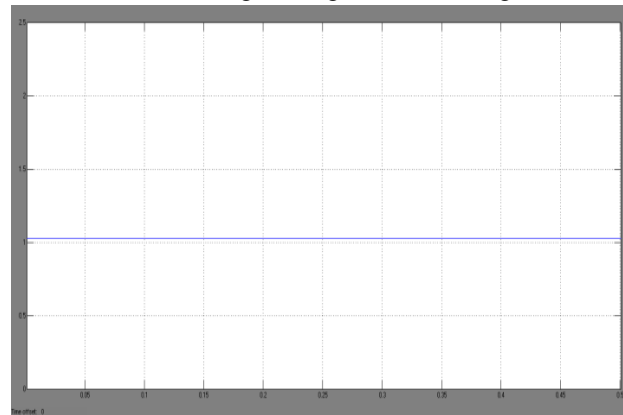
(f) Isabc stator currents



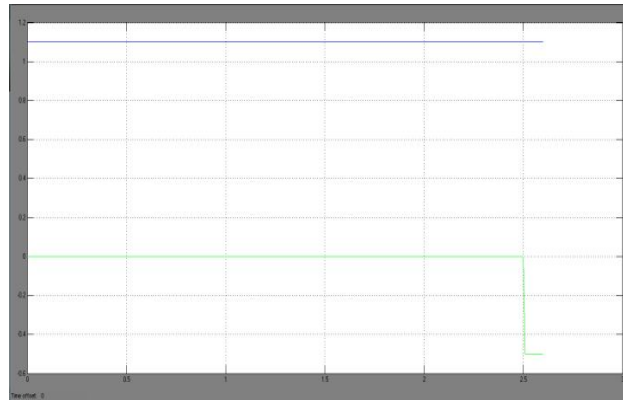
(g) Q_g reactive power injected by the system



(h) Vhdc high voltage DC bus voltage



(i) Vldc low voltage DC bus voltage



(j) Inner loop controlled d-q axis grid currents

Fig 7. Simulation waveforms for Normal operation of proposed configuration showing dynamics of P and Q injection

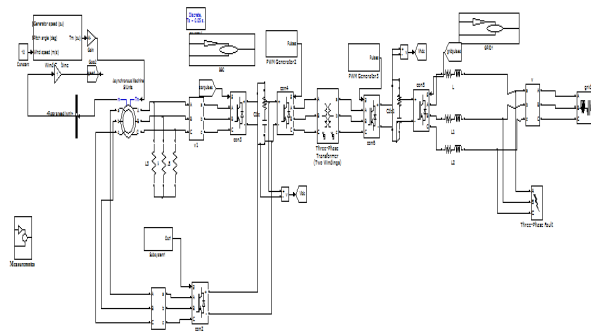
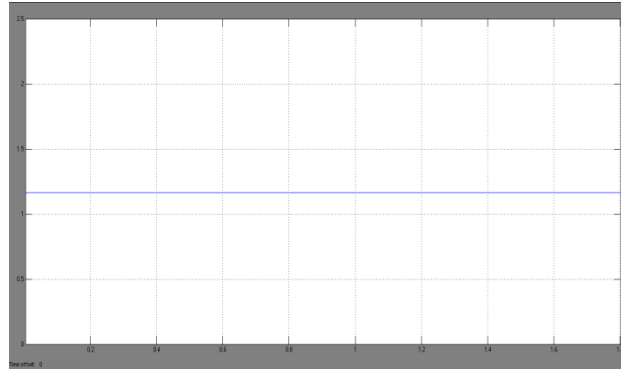
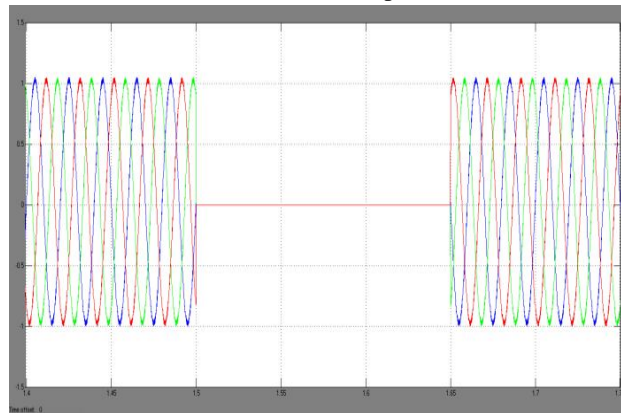


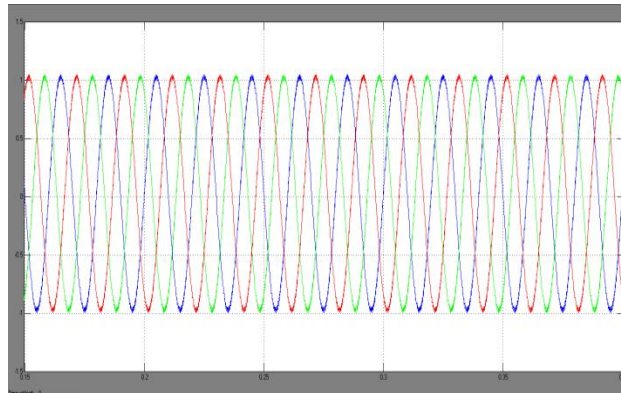
Fig.8 Matlab/Simulink circuit for Proposed SST based DFIG configuration



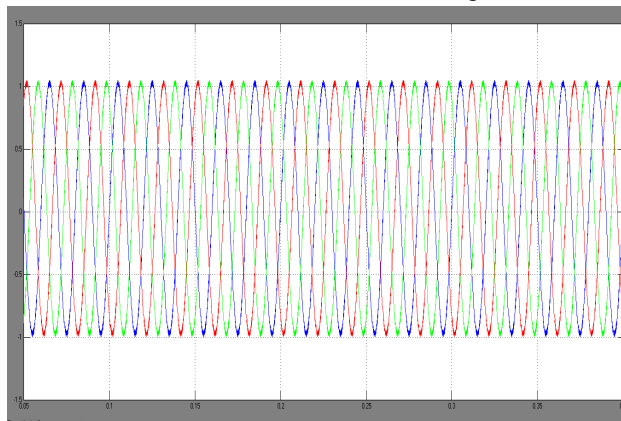
(a) Rotor Speed



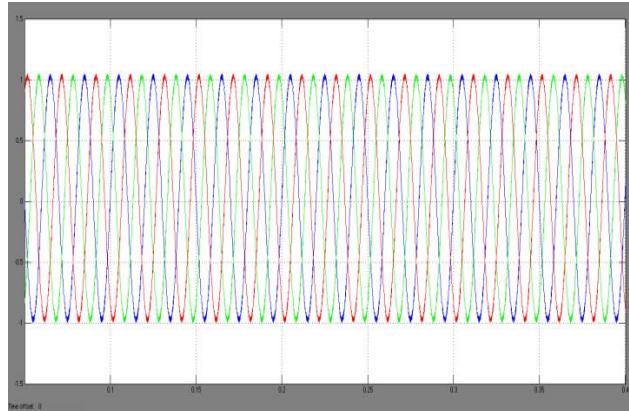
(b) Vgabc Grid Voltages



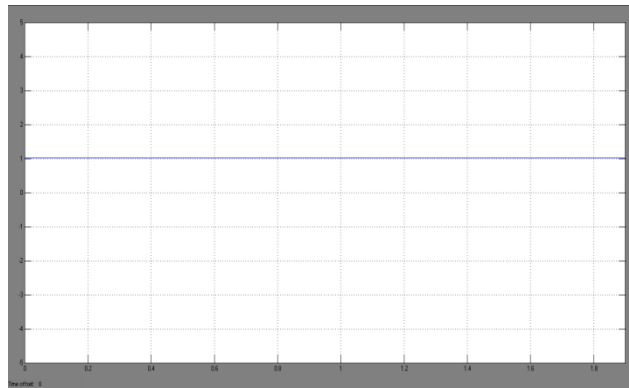
(c) Vsabc Stator terminal voltages



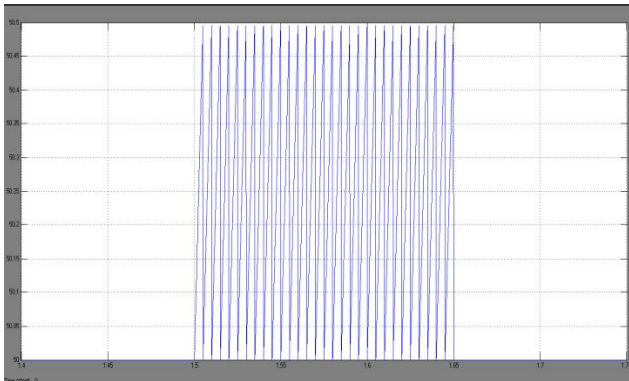
(d) Grid Currents



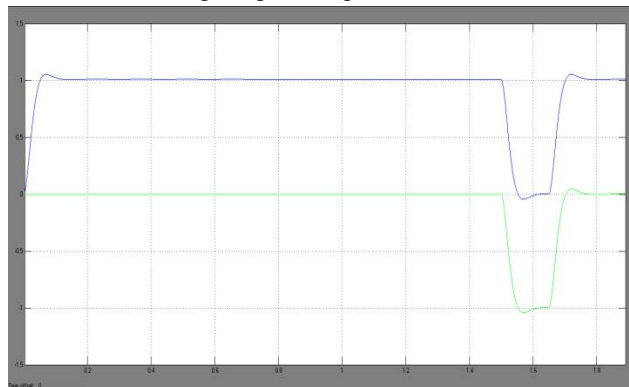
(e) Stator currents



(f) Low voltage DC bus

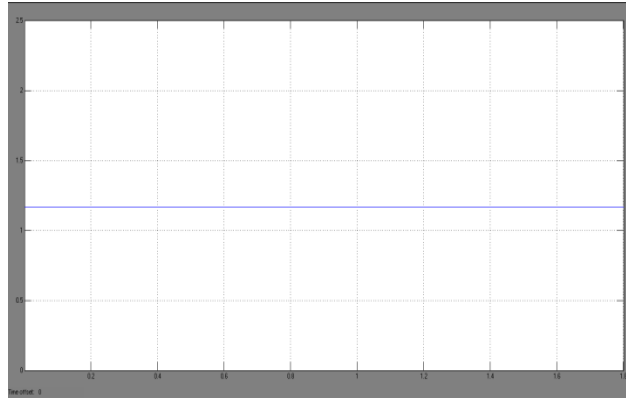


(g) High voltage DC bus

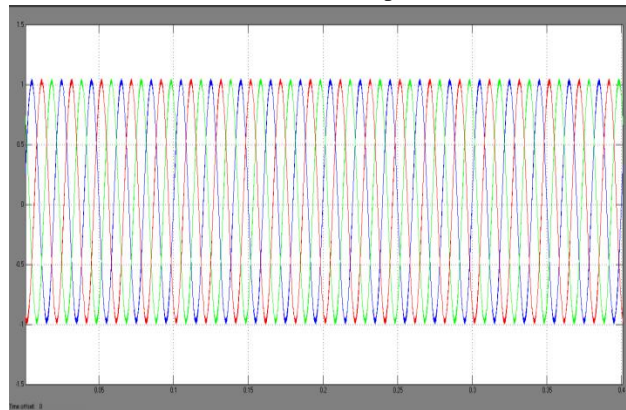


(h) Inner loop controlled d-q axis grid currents,

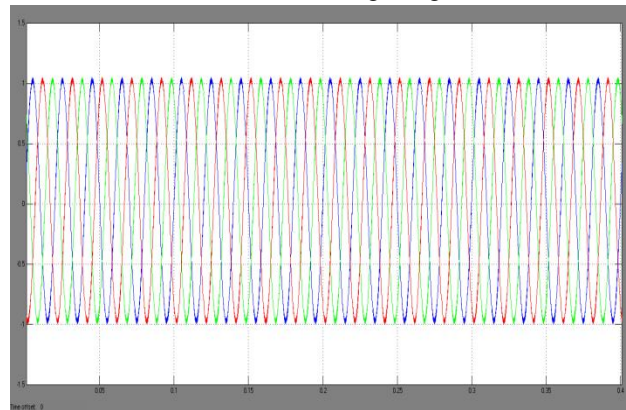
Fig.9. Simulation waveforms for Performance of the proposed configuration under three-phase symmetrical LLL-G fault



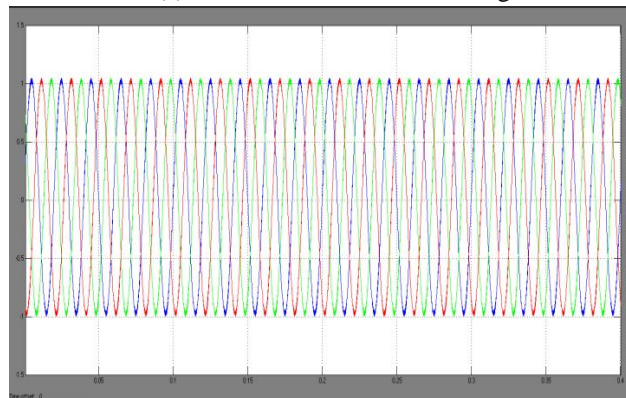
(a) Rotor Speed



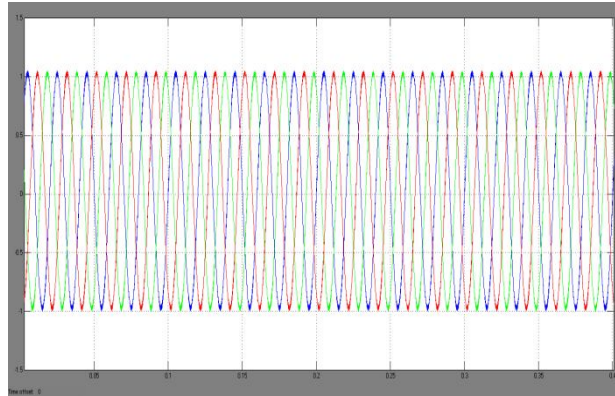
(b) Grid voltages V_{gabc}



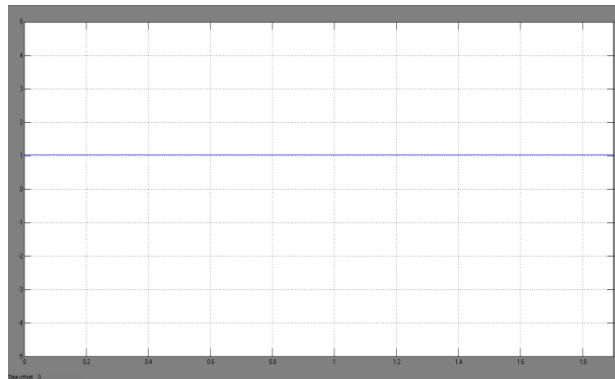
(c) V_{sabc} Stator terminal voltages



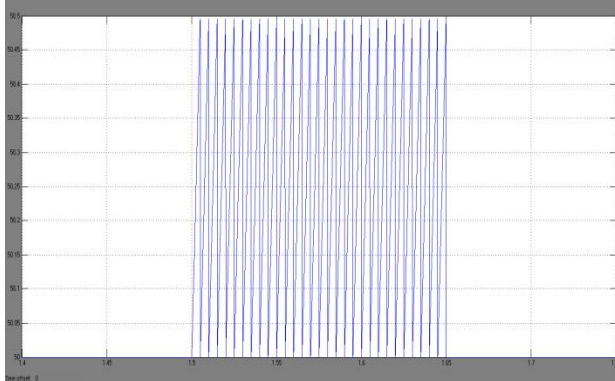
(d) Grid currents I_{gabc}



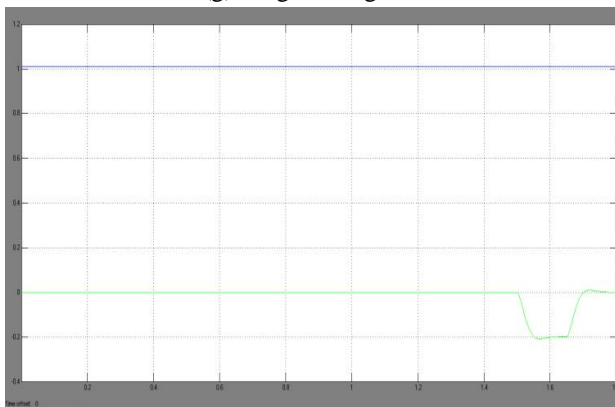
(e) Isabc Stator currents



(f) Vldc Low voltage DC bus

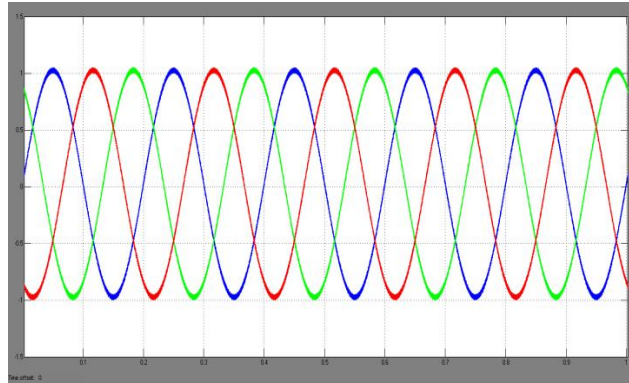


(g) High voltage DC bus

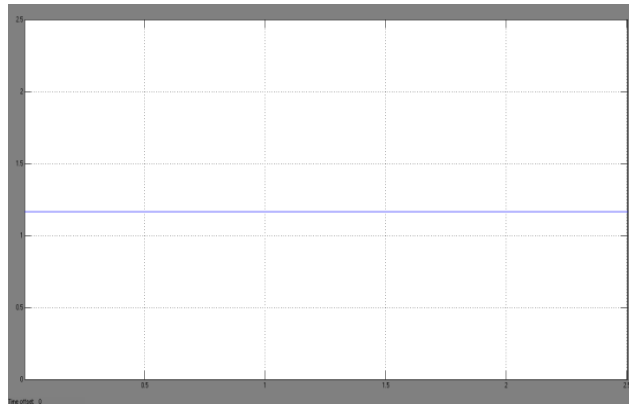


(h) Inner loop controlled d-q axis grid currents

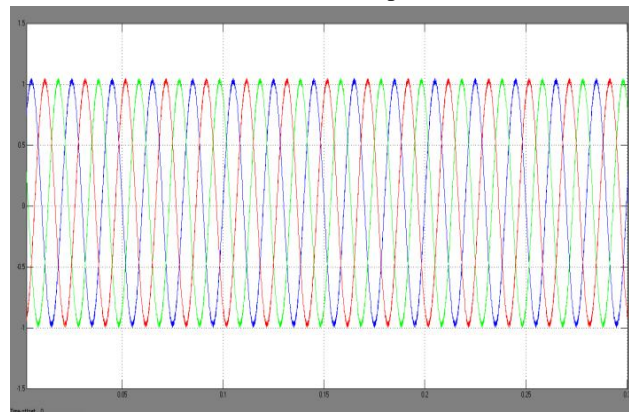
Fig.10. Simulation waveform for Performance of the proposed configuration under three-phase unsymmetrical L-G fault



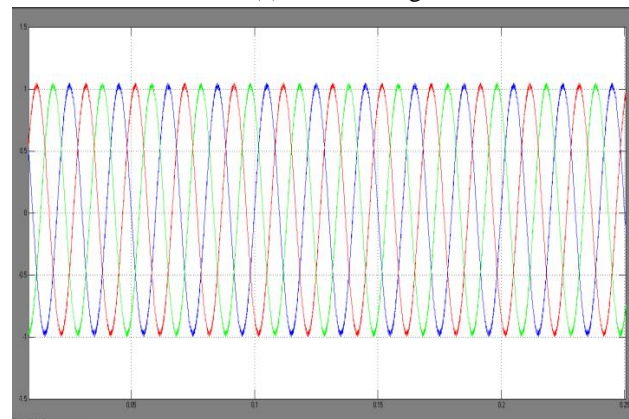
(a) Rotor Currents



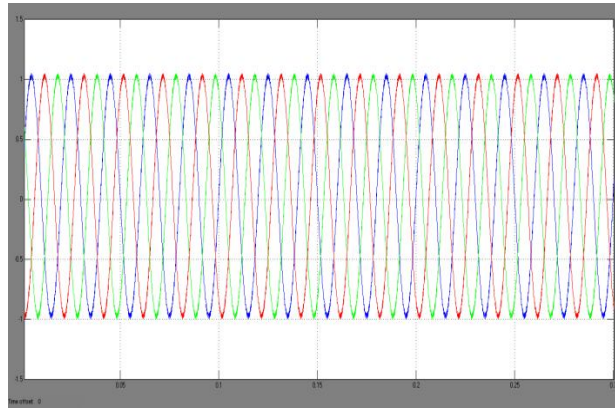
(b) Rotor Speed



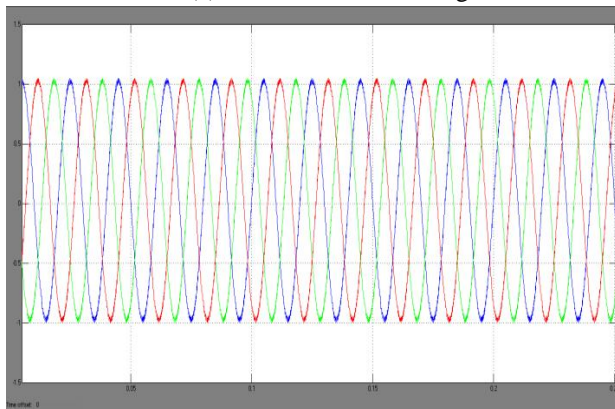
(c) Grid voltages



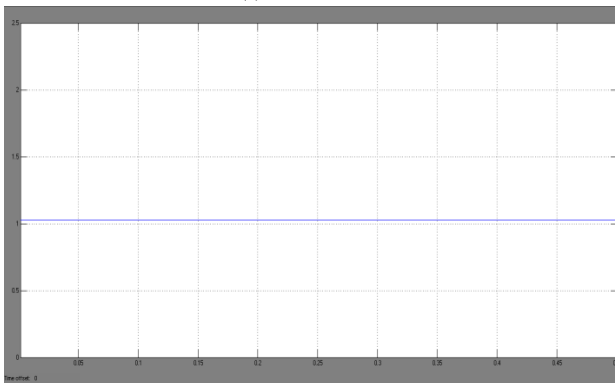
(d) Grid currents



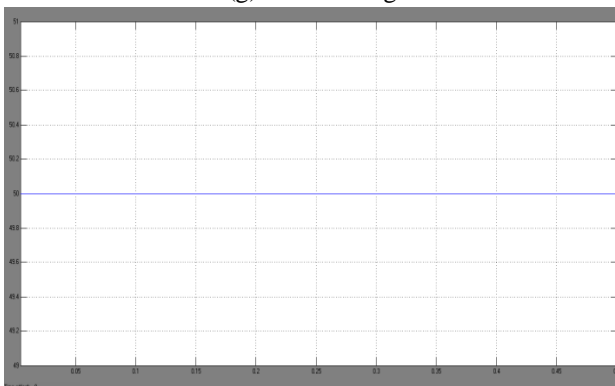
(e) Stator terminal voltages



(f) Stator currents



(g) Low voltage DC



(h) High voltage DC bus

Fig.14. Simulation waveforms for operation of proposed configuration under fault

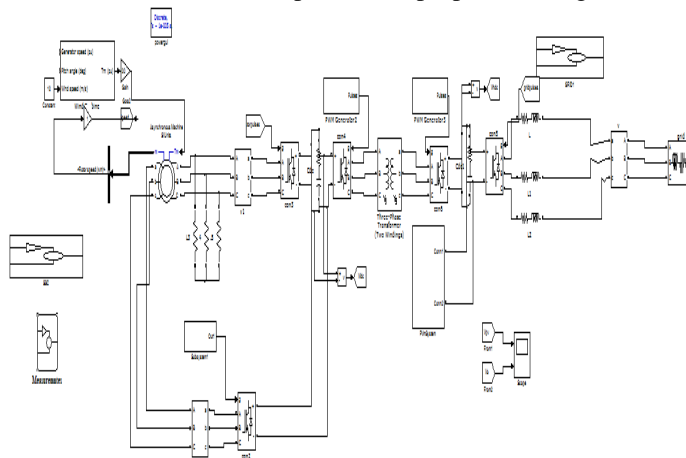


Fig.15. Matlab/Simulink circuit diagram for SST based DFIG configuration with Photovoltaic System

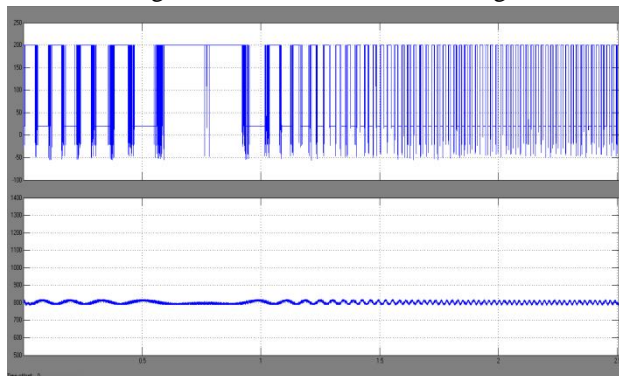


Fig.16. Simulation waveform for PV Voltage and Output voltage

VI. CONCLUSION

In this paper, a new system configuration that combines DFIG and SST operation has been proposed. This configuration replaces the regular fundamental frequency transformer with advanced power electronics based SST. The proposed system is extended with PV and wind based hybrid renewable system for effective operation which observes that SST controls the active power to/from the rotor side converter (RSC), thus, eliminating the grid side converter (GSC) and meets the recent grid code requirements of wind turbine operation under fault conditions. Additionally, it has the ability to supply reactive power to the grid when the wind generation is not up to its rated value.

REFERENCES

- [1] R.Thamaraiselvi, P.Ramesh, J.Baskaran, Sharmeela and G.Kumaresan , “ A Survey of PV Based Solid State Transformer for Storage and Distribution Applications,” International Journal of Scientific & Engineering Research, Volume 4, Issue 12, December-2013 ISSN 2229-5518.
- [2] Dhamodharan Shanmugam, Dhivya Balakrishnan and K.Indiradevi, “Solid State Transformer Integration In Smart Grid System,” International Journal of Science & Technology ISSN (online): 2250-141X www.ijst.co.in Vol. 3 Issue 2, October 2013.
- [3] X. She, A. Q. Huang and R. Burgos, “Review of Solid-State Transformer Technologies and Their Application in Power Distribution Systems,” IEEE J.Emerg. Sel. Topics Power Electronics, vol. 1, no. 3, pp. 186-198, Sept. 2013.
- [4] X. She, X. Yu, F. Wang and A. Q. Huang, “Design and Demonstration of a 3.6-kV–120-V/10-kVA Solid-State Transformer for Smart Grid Application,” IEEE Trans. Power Electron. vol. 29, no. 8, pp. 3982-3996, Aug. 2014.
- [5] Fei Wang, Gangyao Wang, A. Huang, Wensong Yu, Xijun Ni, “Design and operation of A 3.6kV high performance solid state transformer based on 13kV SiC MOSFET and JBS diode,” in Proc. IEEE Energy Conversion Congress and Exposition (ECCE), Sept. 2014.
- [6] J. L. Brooks, “Solid State Transformer Concept Development,” Naval Material Command, Civil Engineering Laboratory, Naval Construction Battalion Ctr., Port Hueneme, CA, 1980.
- [7] J. M. Aga, H. T. Jadhav, “Improving fault ride-through capability of DFIG connected wind turbine system: A review,” in Proc. Int Conf. on Power, Ener. And Control, pp. 613-618, Feb. 2013.



- [8] S. Madhusoodhanan, A. Tripathi, D. Patel, K. Mainali, A. Kadavelugu, S. Hazra, S. Bhattacharya, K. Hatua, "Solid-State Transformer and MV Grid Tie Applications Enabled by 15 kV SiC IGBTs and 10 kV SiC MOSFETs Based Multilevel Converters," in IEEE Trans. Ind. App., vol. 51, no. 4, pp. 3343-3360, July-Aug. 2015.
- [9] L. G. Meegahapola, T. Littler, D. Flynn, "Decoupled-DFIG Fault Ride-Through Strategy for Enhanced Stability Performance During Grid Faults," IEEE Trans. Sust. Energy, vol. 1, no. 3, pp. 152-162, Oct. 2010.
- [10] Y. Jie, Z. Wu and S. Bhattacharya, "Power dispatch strategy in microgrid integrated with solid state transformer," in Proc. IEEE Power Eng. Soc. Gen. Meeting, 2013, pp. 1-5.
- [11] S. Hu, X. Lin, Y. Kang, and X. Zou, "An improved low-voltage ride through control strategy of doubly fed induction generator during grid faults," IEEE Trans. Power Electron., vol. 26, no. 12, pp. 3653-3665, Dec. 2011.
- [12] L. Peng, B. Francois, and Y. Li, "Improved crowbar control strategy of DFIG based wind turbines for grid fault ride-through," in Proc. IEEE 24th Annual Applied Power Electronics Conf. Expo., Washington, DC, USA, Feb. 2009.
- [13] X. She, A. Q. Huang, F. Wang and R. Burgos, "Wind Energy System With Integrated Functions of Active Power Transfer, Reactive Power Compensation, and Voltage Conversion," IEEE Trans. Ind. Electron., vol. 60, no. 10, pp. 4512-4524, Oct. 2013.



10.22214/IJRASET



45.98



IMPACT FACTOR:
7.129



IMPACT FACTOR:
7.429



INTERNATIONAL JOURNAL FOR RESEARCH

IN APPLIED SCIENCE & ENGINEERING TECHNOLOGY

Call : 08813907089  (24*7 Support on Whatsapp)